New Phytologist

Research

Differential phosphorylation of the N-terminal extension regulates phytochrome B signaling

András Viczián[1]*, Éva Ádám[1,2]*, Anne-Marie Staudt[3], Dorothee Lambert[3], Eva Klement[4], Sofia Romero Montepaone[5], Andreas Hiltbrunner[3,6], Jorge Casal[5,7], Eberhard Schäfer[3], Ferenc Nagy[1] and Cornelia Klose[3]

[1]Institute of Plant Biology, Biological Research Centre, Temesvári krt. 62, H-6726, Szeged, Hungary; [2]Research Institute of Translational Biomedicine, Department of Dermatology and Allergology, University of Szeged, H-6726, Szeged, Hungary; [3]Institute of Biology II, University of Freiburg, 79104, Freiburg, Germany; [4]Laboratory of Proteomics Research, Biological Research Centre, Temesvári krt. 62, H-6726, Szeged, Hungary; [5]Instituto de Investigaciones Fisiológicas y Ecológicas Vinculadas a la Agricultura (IFEVA), Facultad de Agronomía, Universidad de Buenos Aires and Consejo Nacional de Investigaciones Científicas y Técnicas (CONICET), C1417DSE, Buenos Aires, Argentina; [6]Signalling Research Centres BIOSS and CIBSS, University of Freiburg, 79104, Freiburg, Germany; [7]Fundación Instituto Leloir, Instituto de Investigaciones Bioquímicas de Buenos Aires, CONICET, C1405BWE, Buenos Aires, Argentina

Author for correspondence:
Cornelia Klose
Tel: +49 761 2036 7868
Email: cornelia.klose@biologie.uni-freiburg.de

Received: *17 July 2019*
Accepted: *24 September 2019*

New Phytologist (2019)
doi: 10.1111/nph.16243

Key words: dark reversion, phosphorylation, phyB NTE, phytochrome, thermal reversion.

Summary

- Phytochrome B (phyB) is an excellent light quality and quantity sensor that can detect subtle changes in the light environment. The relative amounts of the biologically active photoreceptor (phyB Pfr) are determined by the light conditions and light independent thermal relaxation of Pfr into the inactive phyB Pr, termed thermal reversion. Little is known about the regulation of thermal reversion and how it affects plants' light sensitivity.
- In this study we identified several serine/threonine residues on the N-terminal extension (NTE) of *Arabidopsis thaliana* phyB that are differentially phosphorylated in response to light and temperature, and examined transgenic plants expressing nonphosphorylatable and phosphomimic phyB mutants.
- The NTE of phyB is essential for thermal stability of the Pfr form, and phosphorylation of S86 particularly enhances the thermal reversion rate of the phyB Pfr–Pr heterodimer *in vivo*. We demonstrate that S86 phosphorylation is especially critical for phyB signaling compared with phosphorylation of the more N-terminal residues. Interestingly, S86 phosphorylation is reduced in light, paralleled by a progressive Pfr stabilization under prolonged irradiation.
- By investigating other phytochromes (phyD and phyE) we provide evidence that acceleration of thermal reversion by phosphorylation represents a general mechanism for attenuating phytochrome signaling.

Introduction

Plants use photoreceptors to constantly monitor ambient light conditions in order to adjust their growth and development in an ever-changing environment. Red and far-red light is detected by the phytochrome (phy) family of sensory photoreceptors, which in *Arabidopsis thaliana* comprises five members (phyA–E) with different but also partially overlapping functions (Sánchez-Lamas *et al.*, 2016). Phytochromes are synthesized in the red light-absorbing form (Pr) that is, upon exposure to red light, photoconverted into the biologically active far-red light-absorbing form (Pfr) (Rockwell *et al.*, 2006). Light absorption by Pfr in turn induces photoconversion to Pr. The Pfr form is thermally unstable and reverts back into Pr via light-independent thermal reversion, and thus photoconversion and thermal reversion determine the steady-state amount of the active Pfr form. PhyB, the dominant phy in light-grown plants, is a potent light quality and quantity sensor and gradually controls photomorphogenic development (Klose *et al.*, 2015). Upon light exposure, the activated phytochromes translocate into the nucleus where they can localize to subnuclear structures called photobodies (PBs) (Yamaguchi *et al.*, 1999; Kircher *et al.*, 2002). In the nucleus, Pfr interacts specifically with multiple signaling molecules and induces massive transcriptional changes related to the initiation of photomorphogenic development (Quail, 2002).

Phytochromes are composed of an N-terminal photosensory module (PSM) and a C-terminal output module (OPM) connected by a flexible hinge region (Fig. 1a). The PSM consists of an N-terminal extension (NTE), a Per/Arnt/Sim (PAS) domain of unknown function, a cyclic guanosine monophosphate (cGMP) phosphodiesterase/adenylyl cyclase/FhlA (GAF) domain that binds a bilin chromophore and a phytochrome-specific PHY domain that is crucial for the stability of the Pfr conformer (Rockwell *et al.*, 2006; Burgie *et al.*, 2014). The OPM contains

*These authors contributed equally to this work.

two PAS-related domains (PAS-A, PAS-B) and a Histidine Kinase Related Domain (HKRD) and is required for phytochrome dimerization (Nagatani, 2010; Qiu *et al.*, 2017).

Phytochromes function as dimers and the Pfr–Pfr homodimer in the nucleus was proposed to be the active conformer of phyB (Klose *et al.*, 2015). Thermal reversion occurs in two steps: a slower reversion from Pfr–Pfr to the Pfr–Pr heterodimer (k_{r2}) and a much faster reversion from Pfr–Pr to the Pr–Pr homodimer (k_{r1}) (Klose *et al.*, 2015). Both reversion rates display strong temperature dependency in a physiological temperature range, enabling phyB to act as temperature sensor (Jung *et al.*, 2016; Legris *et al.*, 2016). In strong light, Pr-to-Pfr photoconversion is dominant and phyB Pfr–Pfr accumulates to high concentrations that decay slowly after transfer to darkness, enabling, for example,

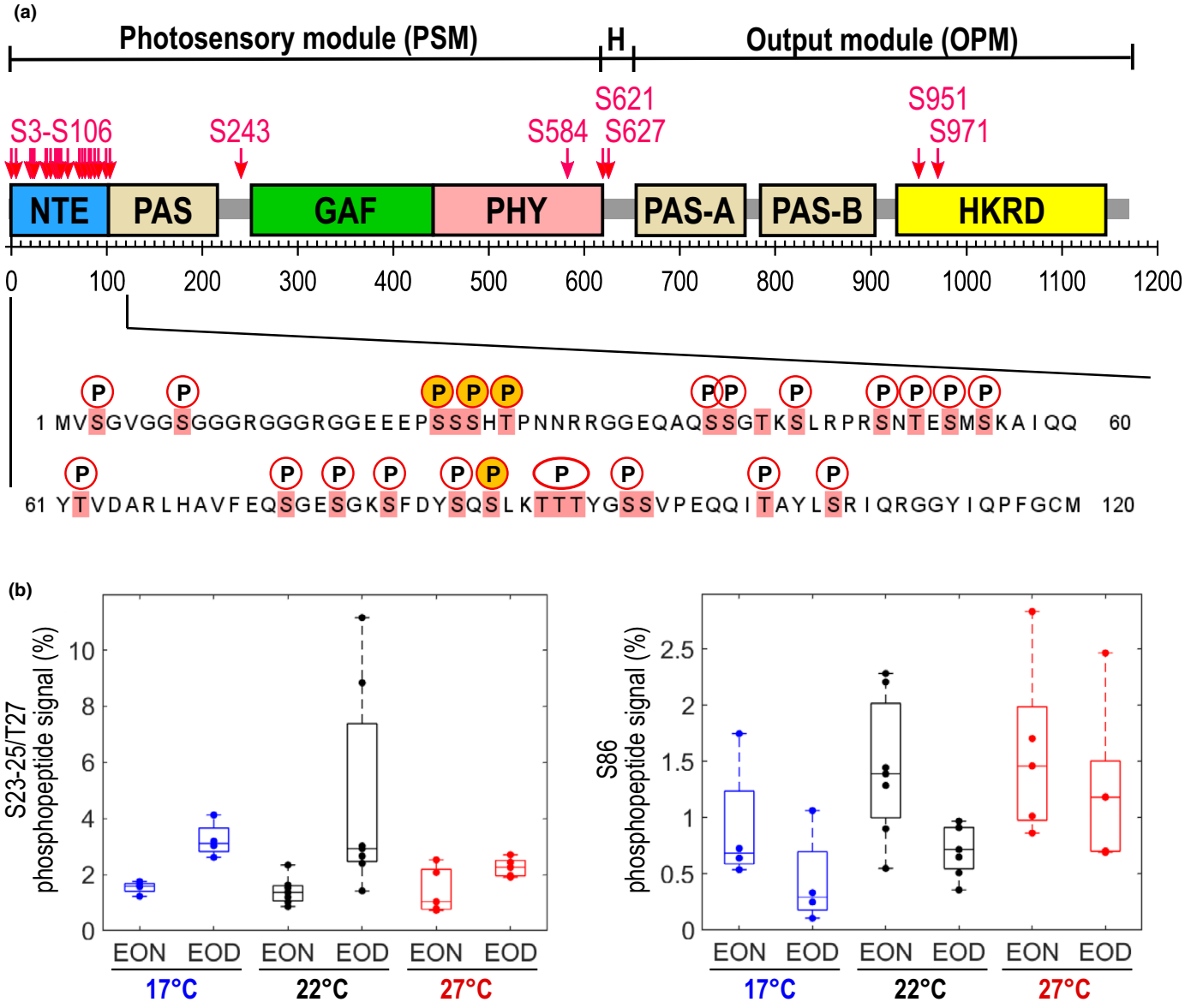

Fig. 1 Identification of phosphorylation sites on *Arabidopsis thaliana* phyB. (a) Schematic representation of the phyB protein structure and the phosphorylation sites identified by MS analysis. Boxes represent protein domains: H, hinge region; NTE, N-terminal extension; PAS, Per/Arnt/Sim domain; GAF, cyclic guanosine monophosphate (cGMP) phosphodiesterase/adenylyl cyclase/FhlA domain; PHY, phytochrome domain; HKRD, Histidin Kinase Related Domain. Red arrows indicate phosphorylated amino acids. Yellow fluorescent protein (YFP)-tagged phyB was immunoprecipitated, digested by trypsin and subjected to phosphopeptide enrichment before MS analysis. Identified phosphorylation sites in the NTE of phyB are shown in detail. All serine and threonine residues are highlighted in red. Phosphorylated residues are labeled with P, light- and temperature-regulated phosphorylation sites are highlighted. (b) Relative phosphopeptide signals corresponding to the fragments containing phosphorylated S23/S25/T27 or phosphorylated S86 amino acid residues, measured in phyB-YFP-expressing plants grown in 12 h : 12 h light : dark cycles at the end of the dark cycle (end of night, EON) or at the end of the light cycle (end of day, EOD) under different temperatures (17, 22 and 27°C). Immunoprecipitated phyB-YFP was trypsin-digested and analyzed by LC-MS/MS. Relative phosphopeptide signals (in %) were calculated from MS1 signal areas and expressed as phosphopeptide signal area divided by the sum of phosphopeptide and unmodified peptide area. Combined box- and scatterplots show the results of biological replicates ($n = 4–7$), and whiskers indicate minimum and maximum datapoints.

night length measurement. In low light conditions, thermal reversion, particularly k_{r1}, becomes increasingly important: it competes with the Pr-to-Pfr photoconversion in determining the amount of Pfr established in a fluence rate-dependent manner. High temperature accelerates k_{r1} and k_{r2}, leading to a decrease of the Pfr concentrations (Jung *et al.*, 2016; Legris *et al.*, 2016).

Previous studies performed in oat found that phytochromes are phosphoproteins acting as autophosphorylating serine/threonine kinases (McMichael & Lagarias, 1990; Lapko *et al.*, 1997; Yeh & Lagarias, 1998; Lapko *et al.*, 1999) and that the kinase domain of phyA is critical for ATP binding and efficient light signaling (Shin *et al.*, 2016). Our knowledge about phosphorylation of *Arabidopsis* phytochromes is rather limited. It was demonstrated, that *Arabidopsis* phyA, phyB and phyD autophosphorylate and have kinase activity towards their interaction partner PHYTOCHROME INTERACTING FACTOR 3 (PIF3) *in vitro* (Shin *et al.*, 2016). Recent reports also showed that Arabidopsis phyA is phosphorylated *in planta* (Zhang *et al.*, 2018; Zhou *et al.*, 2018).

A number of phosphorylated residues in phyB were identified *in vivo*. Whereas phosphorylation of S86 was reported to accelerate thermal reversion, phosphorylation of Y104 was proposed to inhibit binding to PIF3; thus it was suggested that phosphorylation of phyB negatively regulates phyB signaling (Medzihradszky *et al.*, 2013; Nito *et al.*, 2013). Several additional evolutionarily conserved amino acids (S84, T89-91, S106 and Y113) were found to be phosphorylated in a light-dependent manner which locate in the phosphorylation cluster of signaling modulation (PCSM) (Nito *et al.*, 2013). These data suggest that phosphorylation could be a mechanism to modulate phyB signaling.

In this study we examined dynamic phosphorylation at the NTE of phyB in response to light and temperature *in planta* by LC-MS/MS. We investigated the functional role of specific phosphosites using transgenic plants expressing nonphosphorylated and phosphomimic mutants and found that phosphorylation of S86 in phyB's NTE severely alters phyB-mediated red light sensitivity by reducing the amount of physiologically active Pfr. Our data revealed that regulation of thermal reversion by dynamic phosphorylation pattern is particularly important under limiting light conditions where the effect of thermal reversion on red light sensitivity is strong. By investigating phyD and phyE phosphorylation, we provide further evidence that phosphorylation of the PCSM represents a general mechanism for attenuating phytochrome signaling via accelerating thermal reversion.

Materials and Methods

Plant lines and generation of transgenic lines

We used *Arabidopsis thaliana phyB-9* and *phyA-211 phyB-9* mutants in Columbia (Col) and *phyA-2 phyB-1 phyD-1* and *phyA-2 phyB-1 phyE-1* in Landsberg *erecta* (L*er*) background (Reed *et al.*, 1993; Reed *et al.*, 1994; Halliday & Whitelam, 2003).

Arabidopsis lines expressing *35S* promoter-driven phyB-GFP, phyB[S86A]-YFP and phyB[S86D]-YFP in the *phyA-211 phyB-9* background and phyB[G564E]-YFP in *phyB-9* have been described (Ádám *et al.*, 2011; Medzihradszky *et al.*, 2013). Generation of *35S:PHYE-YFP*/*phyABE* and *35S:PHYD-YFP*/*phyABD* lines has been published (Ádám *et al.*, 2013). All other transgenic lines were generated in this study (see Supporting Information Table S1). The *PHYB* promoter was inserted as a *Hind*III/*Xba*I fragment into the p*PCV* vector containing the coding region of the *YELLOW FLUORESCENT PROTEIN* (*YFP*) (Table S2).

The final constructs have been verified by sequencing and transformed into *Arabidopsis* (Clough & Bent, 1998). Homozygous T3 progenies with expression levels comparable to those of the wild-type phyB-expressing lines or the phyE-YFP and phyD-YFP phosphomutants to the corresponding phyE-YFP and phyD-YFP levels were selected for further experiments. Additional independent mutant transgenic lines were also tested and are shown in Figs S1, S4 and S7 (see later), obtaining similar results to those presented in the main text.

Plant sample collection for LC-MS/MS analysis of phyB

Plants were grown on Murashige & Skoog medium (Sigma) containing 3% sucrose for 10 d under an 8 h : 16 h white light : dark regime. Seedlings were collected at the end of the day (EOD) and at the end of the night (EON). The sample preparation and MS analysis are based on Klement *et al.* (2019) and described in detail in the Methods S1.

Plant growth conditions and hypocotyl growth assays

Arabidopsis seeds were sown in Petri dishes on four layers of wet filter paper and stratified for 72 h at 4°C, before they were irradiated with WL for 4 h at 22°C to induce germination and transferred to the dark for 18 h at 22°C. For hypocotyl length measurements seedlings were irradiated with continuous red light (LED; 660 nm) under various temperature conditions for 4 d. Seedlings were placed on agar plates and scanned with a flatbed scanner (Epson, Suwa, Japan). Hypocotyl length was determined using MetaMorph software (Universal Imaging, Downingtown, PA, USA). Relative hypocotyl length was calculated as the ratio of the hypocotyl length of light-grown and the corresponding dark-grown seedlings. The experimental procedure for measurement of hypocotyl growth rates is described in the Methods S1.

Immunoblotting

Thirty micrograms of total protein extracts were separated on 8% sodium dodecyl sulfate-polyacrylamide gel electrophoresis and blotted onto a polyvinylidene fluoride membrane. To detect YFP fusion proteins, the Living Colors A.v. antibody (JL-8; Takara Bio Clontech, Kusatsu, Japan) was used at 1 : 2000 dilution. Actin was detected by the anti-Actin antibody at 1: 10 000 dilution (10-B3; Sigma). A peroxidase-conjugated secondary antibody (31431; Invitrogen) was used at 1 : 10 000 dilution before chemiluminescent signal detection (Medzihradszky *et al.*, 2013).

Epifluorescence microscopy

Epifluorescence microscopy was performed on an Axioplan microscope (Zeiss) using specific filter sets for GFP (Z13, excitation 470 nm, emission 493 nm; Zeiss) and YFP (F31-028, excitation 500 nm, emission 515 nm; AHF Analysentechnik, Tübingen, Germany).

In vivo spectroscopy

For measuring thermal reversion kinetics, 4-d-old etiolated *Arabidopsis* seedlings were irradiated with saturating red light (50 µmol m^{-2} s^{-1} for 20 min at 22°C) to establish the photoequilibrium of 87% Pfr/Ptot (Ptot, total amount of phytochrome), transferred to darkness and kept at either 17, 22 or 27°C. As the *35S:PHYB[S86D]-YFP* line failed to reach the photoequilibrium under this light treatment, we irradiated seedlings for 1 h with 200 µmol m^{-2} s^{-1} on ice in order to increase the Pfr/Ptot value, and transferred them to prewarmed plates in darkness at respective temperatures. Pfr/Ptot was measured using a dual-wavelength ratiospectrophotometer (Klose, 2019) at indicated time points during dark incubation. For steady-state Pfr/Ptot measurements, seedlings were irradiated with red light for 1 h unless otherwise stated and immediately transferred to ice water to minimize Pfr loss during sample handling before measurement. For steady-state Pfr/Ptot measurements in continuous red light, seedlings were grown on ½ MS-agar plates containing 5 µM norflurazon. The herbicide norflurazon (SAN 9789) effectively inhibits carotenoid and Chl accumulation without affecting the phytochrome system (Jabben & Deitzer, 1978; Frosch *et al.*, 1979; Jabben & Deitzer, 1979).

Calculation of the thermal reversion rates k_{r1} and k_{r2}

The thermal reversion rates k_{r2} of each phyB variant and temperature combination were calculated from the measured thermal reversion kinetics using single exponential decay functions. As the calculated k_{r2} exhibited an exponential temperature dependency, k_{r2} was extrapolated for the additional temperatures (4, 12 and 32°C) and used for calculating k_{r1} respectively. The thermal reversion rate k_{r1} was calculated based on the three-state-dimer model (Klose *et al.*, 2015) using the following equation:

$$k_{r1} = \frac{\frac{k_1(2k_2+2k_{r2})+2k_1^2}{Pfr} - 2k_1^2 - 2k_1(2k_2+2k_{r2})}{2k_2+2k_{r2}} - k_2.$$

Results

Detection of phosphorylated amino acids in phyB

To determine phosphorylation sites in phyB, MS analysis of phyB-GFP was performed. *Arabidopsis phyB-9* mutant seedlings expressing *35S:PHYB-GFP* were grown for 10 d under short-day conditions (8 h : 16 h light : dark). The tryptic digest of the phyB-GFP protein, immunoprecipitated using GFP antibody, was enriched for phosphopeptides and subsequently analyzed by LC-MS/MS, which revealed numerous phosphorylated serine (S) or threonine (T) residues predominantly in the N-terminal region of phyB (Fig. 1a; Notes S1). Almost every serine or threonine residue in the NTE was phosphorylated (22 in total between S3 and S106). The analysis confirmed some of the phosphorylation sites reported earlier by Nito *et al.* (2013) on the PCSM-motif of phyB (S84, S86, T89/90/91, S94 and S106), whereas others were not detected in our study (S95, Y104 and Y113). Seventeen phosphorylated residues identified in phyB's NTE have not been explicitly reported previously (S3, S8, S23, S25, T27, S39, S30, S44, S49, T51, S53, S55, T62, S74, S77, S80 and T102). Furthermore we detected one phosphorylated serine (S243) at the beginning of the GAF-domain, one (S584) in the Phy domain, two (S621, S627) in the hinge region and two (S951, S971) in the C-terminal half of phyB (Fig. 1a).

Dynamic phosphorylation at specific serine residues in the NTE of phyB in response to light and temperature

In order to investigate whether phyB phosphorylation changes in response to light and temperature, we grew seedlings expressing phyB-GFP for 10 d in short-day conditions at 17, 22 or 27°C and harvested them at EOD or at EON. For quantitative analyses the tryptic digest of the immunoprecipitated phyB-GFP protein was directly analyzed by LC-MS/MS without phosphopeptide enrichment. Two of the detected phosphorylated phyB fragments exhibited dynamic changes in their phosphorylation status depending on the light and temperature conditions. We observed that the relative phosphopeptide signal of the fragment containing phosphorylated S23/S24/S25/T27 was elevated at the EOD compared with the EON and decreased with temperature rise from 17 to 27°C (Fig. 1b). By contrast, phosphorylation of S86 was higher at EON compared with EOD and elevated temperatures increased phosphorylation in light and darkness (Fig. 1b). These two fragments showed opposite phosphorylation patterns in response to light and temperature.

Impact of temperature and S86 phosphorylation on red light sensitivity

To investigate how S86 phosphorylation modulates light and temperature signaling of phyB, we measured fluence rate response curves for the inhibition of hypocotyl elongation in red light at different ambient temperatures (17, 22 and 27°C). The serine residue at position 86 was substituted with alanine to obtain a nonphosphorylatable mutant phyB[S86A] or with a negatively charged aspartate to mimic a constitutively phosphorylated residue phyB[S86D], as described previously for transgenic lines overexpressing phyB by the *35S* promoter (Medzihradszky *et al.*, 2013). It is well established that phyB signaling is dose-dependent (Wagner *et al.*, 1991), therefore we generated lines expressing the phyB, phyB[S86A] and phyB[S86D] fused to YFP under the control of the native *PHYB* promoter in the *phyB-9* mutant at comparable levels to the endogenous phyB in Col-0 wild-type (WT). The phyB[S86D] mutant exhibited a strong

hyposensitive phenotype in red light compared with phyB, whereas phyB[S86A] was hypersensitive under all tested temperatures (Figs 2a–c, S1), although phyB[S86D] was considerably more highly expressed (Figs 2d, S1). The red light responsiveness of all three genotypes was progressively reduced with increasing temperatures. Interestingly, the differences in red light sensitivity between the examined lines were obvious at fluence rates below 5 $\mu mol\ m^{-2}\ s^{-1}$ but they exhibited similar responses at higher fluence rates (Fig. 2a–c).

Impact of temperature and S86 phosphorylation on Pfr steady-state concentrations in light

The phyB activity depends on the amount of phyB in the Pfr–Pfr homodimer conformation (Klose *et al.*, 2015). Whereas thermal reversion from the Pfr–Pfr to Pfr–Pr occurs at a slow rate, k_{r2}, the thermal reversion rate, k_{r1}, from Pfr–Pr to Pr–Pr is much faster. In limiting light conditions and high temperatures, thermal reversion, especially k_{r1}, becomes increasingly important for the irradiance and temperature dependence of phyB activity (Sellaro *et al.*, 2019). It has been reported that the phosphomimic phyB [S86D] mutant has accelerated thermal reversion after transfer from light to darkness, and this is mainly a result of the slow reversion rate, k_{r2}, that has a minor impact on Pfr concentrations in light and thus cannot directly account for the hyposensitivity of phyB[S86D] seedlings in red light (Medzihradszky *et al.*, 2013).

Here, we wanted to investigate the extent to which the fast reversion rate k_{r1} is affected by S86 phosphorylation. Therefore, we determined the Pfr concentration relative to the total phytochrome amount (Pfr/Ptot) in steady-state conditions for phyB, phyB[S86A] and phyB[S86D] in different light intensities and temperatures by *in vivo* spectroscopy. As physiological phyB levels are too low for detection, we used lines overexpressing phyB, phyB[S86A] or phyB[S86D] fused to YFP by the *35S* promoter in a *phyA-211 phyB-9* double mutant background. Steady-state Pfr/Ptot ratios for phyB measured *in vivo* showed strong fluence rate dependence in the range 0.5–5 $\mu mol\ m^{-2}\ s^{-1}$ of red light (Fig. 2e). PhyB[S86A] can establish Pfr/Ptot values comparable to WT phyB in two- to three-fold lower red fluence rates, which is consistent with its hypersensitive phenotype. By contrast, much higher red light intensities had to be applied to reach equivalent Pfr/Ptot ratios for phyB[S86D], which is in agreement with the strongly impaired red light sensitivity of the phyB [S86D] mutant. Even 100 $\mu mol\ m^{-2}\ s^{-1}$ red light was not sufficient to establish the photoequilibrium of 87% Pfr/Ptot, indicating that the phyB[S86D] Pfr–Pr form is thermally highly unstable. We detected a strong temperature dependence of the steady-state Pfr/Ptot values under nonsaturating light conditions for all three different genotypes showing reduced relative Pfr concentrations at elevated temperatures (Fig. 2f).

To calculate the thermal reversion rates k_{r1} and k_{r2} we additionally obtained temperature-dependent thermal reversion kinetics for phyB, phyB[S86A] and phyB[S86D]. Consistent with previous findings (Medzihradszky *et al.*, 2013) the S86D mutation showed accelerated thermal reversion kinetics, whereas S86A exhibited slower thermal reversion kinetics at all tested temperatures (Fig. S2). In addition, all lines showed a strong temperature dependence, displaying faster thermal reversion at higher temperatures. Thermal reversion is usually efficiently suppressed at low temperatures, but even at 4°C the phyB[S86D] mutant exhibited fast and complete reversion comparable to the kinetics measured in the WT at 27°C (Fig. S2). We calculated the thermal reversion rates k_{r1} and k_{r2} (Fig. 2g–i): k_{r1} was reduced two- to three-fold for phyB[S86A] compared with phyB, but about 50-fold increased for phyB[S86D], which correlates with the measured fluence rate dependence of the relative Pfr/Ptot values (Fig. 2e,h). Interestingly, k_{r1} of all three phyB versions showed equal temperature dependence (Fig. 2h), indicating that S86 phosphorylation is not the only mechanism affecting k_{r1} and that temperature dependency of thermal reversion represents instead an intrinsic property of the chromophore.

PhyB Pfr is stabilized under prolonged irradiation

We noticed that the fluence rate range of the phyB-mediated physiological response was much broader compared with the one of the measured steady-state Pfr/Ptot ratios. Transgenic seedlings expressing WT phyB responded strongly to light below 1 $\mu mol\ m^{-2}\ s^{-1}$, whereas the measured Pfr/Ptot values were < 20% (Fig. 2b,e). Also the phyB[S86D] mutant responded to red light below 10 $\mu mol\ m^{-2}\ s^{-1}$ but possesses hardly any detectable Pfr (Fig. 2b,e). The reason for this discrepancy could be a consequence of the differential experimental conditions used: hypocotyl growth inhibition was monitored after 4 d of growth in continuous light, whereas Pfr/Ptot was measured in etiolated seedlings after 1 h red light treatment. Thus we determined steady-state Pfr/Ptot values in seedlings grown for up to 3 d in continuous red light. As Chl interferes with the *in vivo* spectroscopic measurements, seedlings were grown on medium containing 5 μM norflurazon to bleach the chloroplasts. After 1 h red light treatment, etiolated seedlings grown on norflurazon established Pfr/Ptot values comparable to seedlings grown in standard conditions, indicating that the norflurazon treatment does not affect Pfr/Ptot (Figs 2e, 3a–c). However, after 3 d of irradiation, Pfr/Ptot ratios were considerably higher compared with 1 h or 1 d, indicating a progressive Pfr stabilization in light (Fig. 3a,b). Seedlings expressing phyB or phyB[S86D] that received a Pfr-reverting far-red light pulse after 3 d of red irradiation and subsequently were irradiated with 1 h red light established the same high Pfr/Ptot values, demonstrating that the steady state is established within 1 h of light treatment (Fig. 3c). Furthermore, the Pfr stabilization of phyB[S86D] was less pronounced compared with phyB, indicating that this phenomenon is also regulated, at least partially, by phosphorylation.

Pfr/Ptot ratios measured under prolonged irradiation nicely matched the fluence rate response curves at lower fluence rates. After 3 d of irradiation, full photoequilibrium was established in plants expressing phyB[S86A] at 1 $\mu mol\ m^{-2}\ s^{-1}$ (Fig. 3a) while their red light response reached a plateau (Fig. 2b), which was less pronounced for WT phyB that still reaches > 60% Pfr/Ptot at 1 $\mu mol\ m^{-2}\ s^{-1}$ (Fig. 2b). Expressing phyB[S86D] resulted in

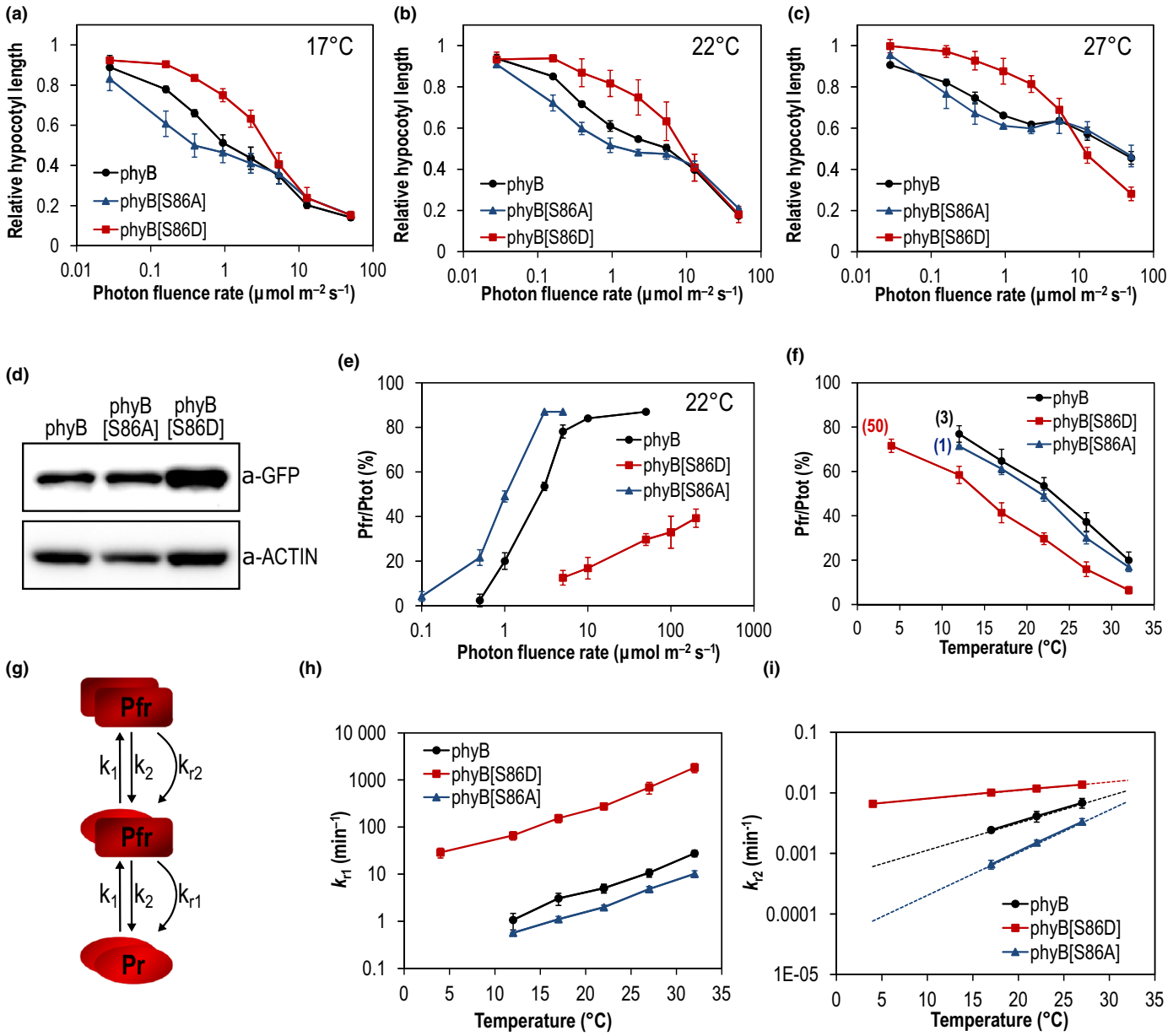

Fig. 2 phyB S86 phosphorylation modulates red light sensitivity of *Arabidopsis thaliana* by altering concentrations of the far-red light-absorbing form (Pfr) of phytochrome B in light. (a–c) Fluence rate response curves for the inhibition of hypocotyl elongation in red light at 17°C (a), 22°C (b) and 27°C (c). Seedlings expressing physiological levels of phyB-yellow fluorescent protein (phyB-YFP), phyB[S86A]-YFP or phyB[S86D]-YFP in the *phyB-9* mutant background were grown for 4 d in continuous red light. Relative hypocotyl lengths were calculated to the length of the corresponding dark controls. Data are means of two biological replicates with $n \leq 60$ seedlings. Error bars indicate SEM. (d) Immunoblot of total protein extracts from 4-d-old dark-grown seedlings of the transgenic lines used in (a–c). The phyB-YFP fusion proteins were detected using monoclonal anti-GFP antibody. Actin was used as loading control. (e, f) Relative Pfr/Ptot ratios (Ptot, total amount of phytochrome) established under steady-state conditions in different fluence rates of red light at 22°C (e) or different temperatures but constant fluence rates (f) were measured by *in vivo* spectroscopy. The red light intensities used for irradiation in (f) are indicated in brackets and given in µmol m^{-2} s^{-1}. Seedlings overexpressing phyB-GFP, phyB[S86A]-YFP or phyB[S86D]-YFP in the *phyA-211 phyB-9* double mutant background were grown for 4 d in darkness and irradiated for 1 h with red light before measurement. Relative Pfr concentrations (%) are calculated based on Ptot. Data are means of $n \geq 3$ independent measurements. Error bars represent SEM. (g) Schematic representation of the three-state phytochrome dimer model. The photoconversion rates k_1 (Pr to Pfr) and k_2 (Pfr to Pr) as well as the thermal reversion rates k_{r1} (Pfr–Pr to Pr–Pr) and k_{r2} (Pfr–Pfr to Pfr–Pr) are depicted with arrows. (h, i) The temperature dependence of the thermal reversion rates k_{r1} (h) and k_{r2} (i) was calculated using data shown in (f) and in Supporting Information Fig. S1. Error bars represent SEM. Dotted lines in (i) represent exponential trend lines used to extrapolate values for calculation of k_{r1} at additional temperature values.

similar hypocotyl growth inhibition at *c.* 10 µmol m^{-2} s^{-1} but seedlings only accumulated < 40% Pfr/Ptot (Fig. 3b); however, the response could have been compensated by the higher phyB [S86D] expression level (Fig. 2d). This indicates that the irradiance-sensitive physiological response at higher fluence rates (> 10 µmol m^{-2} s^{-1}) is independent of S86 phosphorylation and

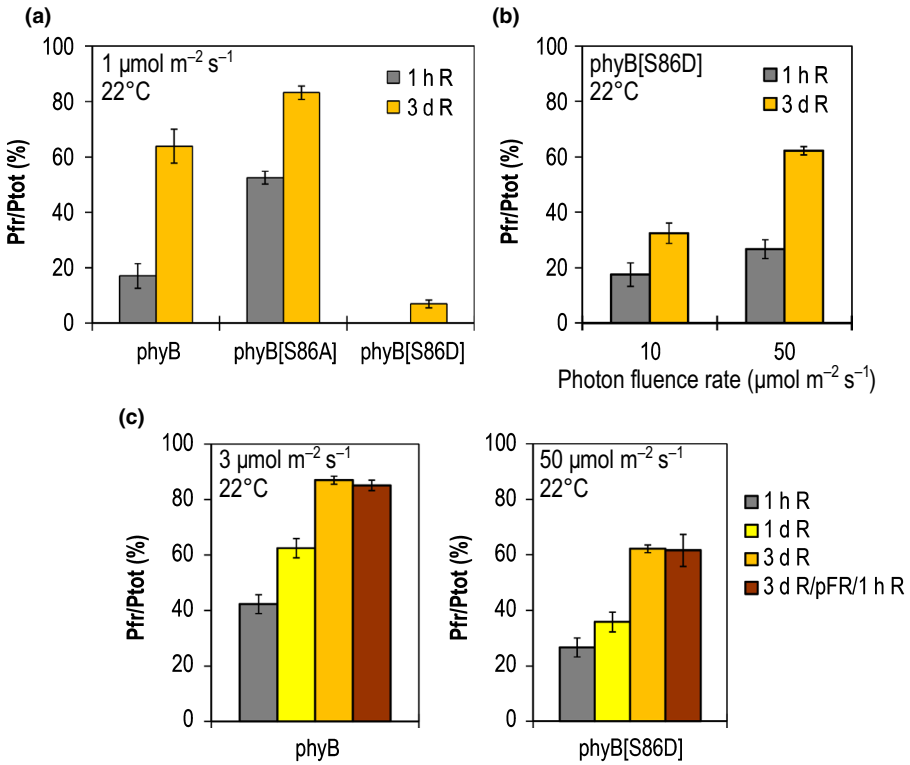

Fig. 3 The far-red light-absorbing form (Pfr) of phyB is stabilized in continuous red light in *Arabidopsis thaliana*. (a–c) Pfr/Ptot ratios (Ptot, total amount of phytochrome) established under prolonged irradiation with red light at 22°C were measured by *in vivo* spectroscopy. Seedlings were grown on norflurazon-containing plates. (a) Seedlings overexpressing phyB-green fluorescent protein (phyB-GFP), phyB[S86A]-yellow fluorescent protein (phyB[S86A]-YFP) or phyB[S86D]-YFP in the *phyA-211 phyB-9* double mutant background were grown for 1 d in darkness followed by 3 d in 1 µmol m^{-2} s^{-1} red light (3 d R). As a control, 4-d-old etiolated seedlings were irradiated for 1 h with 1 µmol m^{-2} s^{-1} red light (1 h R). (b) Seedlings overexpressing phyB[S86D]-YFP were grown for 1 d in darkness followed by 3 d in 10 or 50 µmol m^{-2} s^{-1} red light (3 d R). As controls, 4-d-old etiolated seedlings were irradiated with 10 or 50 µmol m^{-2} s^{-1} red light for 1 h (1 h R). (c) Seedlings overexpressing phyB-GFP or phyB[S86D]-YFP were grown for either 3 d in darkness followed by 1 d in 3 or 50 µmol m^{-2} s^{-1} red light (1 d R) or for 1 d in darkness and 3 d in red light (3 d R) or were subsequently treated with a Pfr-reverting far-red light pulse (776 nm, 10 min, 50 µmol m^{-2} s^{-1}) followed by 1 h red light irradiation (3 d R/pFR/1 h R). As a control, 4-d-old etiolated seedlings were irradiated with red light for 1 h (1 h R). Data are means of $n \geq 3$ independent measurements. Error bars indicate SEM.

cannot be explained solely by the effect of the thermal reversion of the Pfr–Pr heterodimer on Pfr/Ptot ratios.

The accumulation of phyB in PBs is strictly Pfr-dependent and can be used to monitor the Pfr content (Klose *et al.*, 2015; Legris *et al.*, 2016). Our microscopic analyses revealed that the PB formation is correlated with the measured Pfr/Ptot values, confirming the stabilization of Pfr under prolonged irradiation (Fig. S3). Although WT phyB does not form detectable PBs after 6 h of light treatment, they could be well observed after 3 d of continuous 1 µmol m^{-2} s^{-1} irradiation. This light fluence could not induce PB formation of the phyB[S86D] mutant even after 3 d of irradiation, but 10 µmol m^{-2} s^{-1} of red light illumination for 3 d was necessary to detect the appearance of PBs containing phyB[S86D] (Fig. S3).

PhyB S86 phosphorylation affects growth rate under simulated natural growth conditions

Under natural conditions, a major function of phyB is to sense shade signals arising from competing neighbors, characterized by low red : far-red (R : FR) ratio (Smith, 2000). Shade directly alters the photoconversion rates, favoring the formation of Pfr–Pr heterodimers. In turn, temperature affects the Pfr–Pr thermal reversion rate k_{r1}, a major determinant of light sensitivity (Klose *et al.*, 2015; Sellaro *et al.*, 2019). As k_{r1} strongly depends on S86 phosphorylation (Fig. 2h), we investigated the response to shade at different temperatures in de-etiolated seedlings expressing YFP-fused phyB, phyB[S86A] and phyB[S86D]. The seedlings were grown under diurnal white-light cycles (10 h : 14 h light : dark, 22°C) for 3 d and then transferred to 12 different combinations of shade and temperature during the photoperiod of the fourth day to measure the growth rate of the hypocotyl during that period. The experimental setup is optimal to determine effects on k_{r1}, which is important for growth responses during the day. The Col WT was included under the same conditions and its growth rate was used as a biologically meaningful quantification of the integrated impact of the shade and temperature combinations. We observed the lowest growth rate under white light (R : FR = 1.0) at the lowest temperature (17°C) and the highest growth rates under deep shade (R : FR = 0.1) combined with the highest temperature (28°C) for all tested lines (Fig. 4a,b). As expected, when plotted against the growth rate of the Col WT, the regression line corresponding to the *PHYB:PHYB-YFP* was close to the 1 : 1 line and that corresponding to

the *35S:PHYB-YFP* (phyB overexpressor) was below the 1 : 1 line, owing to stronger phyB-mediated growth inhibition (Fig. 4a,b). In both cases, the slope of the regression line belonging to phyB[S86D] expressors was significantly steeper and that of the phyB[S86A]-expressing plants was less pronounced than their respective transgenic control expressing phyB (Fig. 4a,b). These results indicate that the degree of S86 phosphorylation significantly affects the function of phyB as a sensor of neighbor and temperature cues. Furthermore, the distortion caused by genetic modification of the S86 phosphorylation status was particularly large when the plants were exposed to the combination of increased degrees of shade and high temperatures.

Phosphorylation of serine residues in the NTE of phyD and phyE

PhyD and phyE are evolutionarily related to phyB, and thus we decided to examine the phosphorylation pattern of phyD and of phyE *in planta*. Interestingly, our LC-MS/MS analyses revealed phosphorylation of only single serine residues in the NTE of phyD (S79 or S82) and phyE (S53) (Fig. 5a; Notes S2). Serine residues in close proximity to the identified phosphorylation sites, phyD S88 and phyE S50, are homologous to the conserved S86 of phyB (Fig. 5a). To analyze the effect of phosphorylation of these serines, we generated and examined phyD-YFP or phyE-YFP overexpression lines in *phyABD* or *phyABE* triple mutant background, respectively.

The nonphosphorylatable phyD mutants phyD[S82A] and phyD[S88A] displayed a hypersensitive red light response compared with phyD (Figs 5b–d, S4), although expression levels of these lines were lower (Fig. S5). The phosphomimic phyD [S88D], by contrast, exhibited a reduced red light responsiveness (Figs 5b–d, S4). Along with these results we noticed that the S-to-A mutants of phyD have stronger preference to localize in PBs than the WT or the S-to-D mutant counterparts, indicating that these structures contribute to signaling (Fig. S5). The red light responses of all lines were gradually reduced with increasing temperature, indicating that thermal reversion of phyD could be responsible for light and temperature dependence of the response. Astonishingly, the amounts of photoreversible phyD we detected in the *in vivo* spectroscopic assay were too low to allow precise Pfr estimation, despite the fact that we were using strong phyD overexpressor lines. This suggests that phyD could be highly thermally unstable in the Pfr form and hence circumvent detection in our system. Nevertheless, preventing phosphorylation at the NTE enhanced red light sensitivity of phyD, indicating slightly enhanced Pfr thermal stability.

The phyE overexpression line showed a mild hypocotyl growth inhibition in red light that was not fluence rate-dependent (Figs 5e–g, S4), in good agreement with published data (Ádám *et al.*, 2013). PhyE Pfr proved to be highly thermally stable, without showing detectable thermal reversion within 4 h of darkness (Fig. 5h) and hence accumulated high Pfr concentrations close to the photoequilibrium already at very low red light intensities (0.1 μmol m^{-2} s^{-1}) where phyB did not show any detectable Pfr (Fig. 5i), which explains the lack of fluence rate dependency. The nonphosphorylatable phyE[S50A] mutant was also thermally stable (Fig. 5h) and exhibited a physiological response similar to phyE (Fig. 5e–g). By contrast, the phosphomimic phyE[S50D] mutant was almost blind to red light and showed almost complete thermal reversion within 4 h (Fig. 5e–g). It is interesting to note that phyE and the nonphosphorylatable mutant versions have relatively shorter hypocotyls at higher temperature, which could indicate higher physiological activity or higher stability of

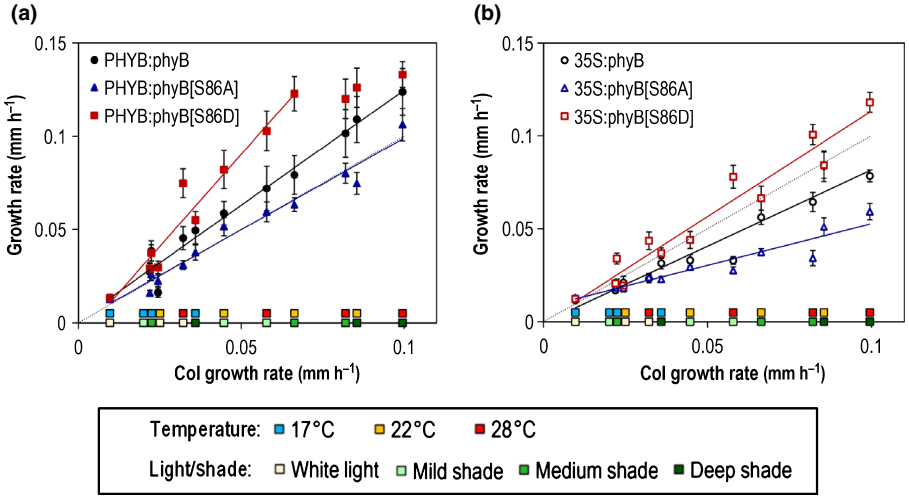

Fig. 4 phyB S86 phosphorylation modulates *Arabidopsis thaliana* seedling growth rate under different shade and temperature combinations. Seedlings expressing phyB-yellow fluorescent protein (phyB-YFP), phyB[S86A]-YFP or phyB[S86D]-YFP from the endogenous *PHYB* promoter (a) in the *phyB-9* mutant background or from the *35S* promoter (b) in the *phyA-211 phyB-9* double mutant background were grown under 10 h : 14 h light : dark regime for 4 d. Twelve different combinations of shade and temperature were applied during photoperiod of day 4. Growth rates were calculated based on the measured hypocotyl length values at the beginning and the end of the light period of day 4. Shade and temperature conditions are represented by colored boxes. The growth rates for the Col wild-type are shown on the *x*-axis. For comparison with the Col wild-type, the corresponding 1 : 1 line is shown as a dotted, black line. Data are means of 12 replicates with $n \leq 120$ seedlings. Error bars indicate SEM.

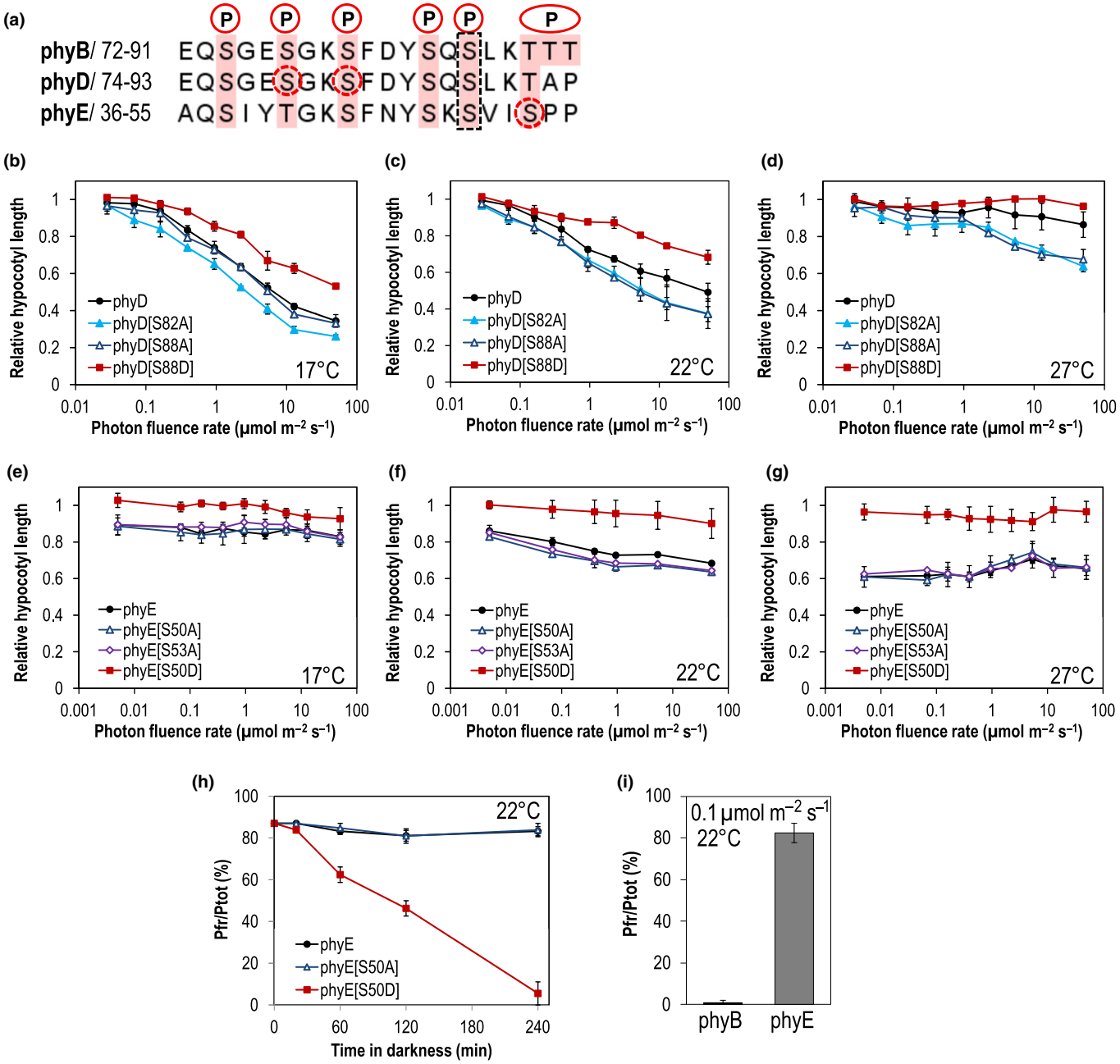

Fig. 5 Phosphorylation at the N-terminal extension (NTE) of phyD and phyE regulates light signaling in *Arabidopsis thaliana*. (a) Alignment of phyB, phyD and phyE amino acid sequences around phyB S86. All serine and threonine residues are highlighted in red and residues phosphorylated in phyB are labeled with P. Phosphorylated serine residues identified by MS analyses in phyD (S79 or S82) and phyE (S53) are indicated with red dashed circles. Serine residues homologous to conserved S86 in phyB are indicated with a black dashed rectangle (phyD S88 and phyE S50). (b–g) Fluence rate response curves for the inhibition of hypocotyl elongation in red light at 17 (b, e), 22 (c, f) and 27°C (d, g). Seedlings expressing phyD-yellow fluorescent protein (phyD-YFP), phyD[S82A]-YFP, phyD[S88A]-YFP or phyD[S88D]-YFP in the *phyABD* mutant background (b–d) or seedlings expressing phyE-YFP, phyE[S50A]-YFP, phyE[S53A]-YFP or phyE[S50D]-YFP in the *phyABE* mutant background (e–g) were grown in continuous red light for 4 d. Relative hypocotyl lengths were calculated to the length of the corresponding dark controls. Data are means of two biological replicates with $n \leq 60$ seedlings. Error bars represent SEM. (h) Thermal reversion kinetics of phyE-YFP-, phyE[S50A]-YFP- and phyDES50D]-YFP-expressing seedlings in the *phyABE* mutant measured by *in vivo* spectroscopy. Four-day-old etiolated seedlings were treated with saturating red light for 20 min before transfer to darkness and relative Pfr/Ptot values (ratio of far-red light-absorbing form of phytochromes (Pfr) to total amount of phytochromes) were measured after 20, 60, 120 and 240 min incubation in the dark at 22°C. Data are means of $n \geq 3$ independent measurements. Error bars indicate SEM. (i) Relative Pfr/Ptot ratios were measured by *in vivo* spectroscopy. Four-day-old etiolated seedlings expressing phyB-GFP in the *phyA-211 phyB-9* mutant or phyE-YFP in the *phyABE* mutant were irradiated for 2 h with 1 µmol m^{-2} s^{-1} red light before measurement. Relative Pfr concentrations (%) are calculated based on Ptot. Data are means of $n \geq 3$ independent measurements. Error bars indicate SEM.

the Pfr form under these conditions. In good agreement with the results of Ádám *et al.* (2013), we found that phyE does not form PBs after extended red irradiation and thus we speculate that they are not required for phyE signaling (Fig. S6). Taken together, these data indicate that phosphorylation at the NTE could be a general mechanism to attenuate light sensitivity of phytochromes by accelerating thermal reversion.

The NTE is essential for Pfr thermal stability

The NTE of phyB has been shown to be important for Pfr thermal stability *in vitro* (Burgie *et al.*, 2014; Burgie *et al.*, 2017), but the physiological relevance of phyB without NTE in *Arabidopsis* has not yet been examined. An *Arabidopsis* line expressing truncated phyB lacking the N-terminal 89-amino-acid phyB[dN89] fused to YFP displayed strongly impaired red light responsiveness as manifested in hyposensitivity for hypocotyl growth inhibition, despite the fact that the expression level of phyB[dN89] was considerably higher than that of the control line (Figs 6a,b, S7). The hyposensitive phenotype of phyB[dN89] was much more severe than that of the phyB[S86D] mutant and correlated with further reduced steady-state Pfr/Ptot values (Fig. 6c). This indicates that thermal stability of the Pfr–Pr heterodimer is dramatically compromised in phyB[dN89].

Multiple phosphorylated residues within the NTE influence phyB signaling

We investigated whether phosphorylation of serine residues in the NTE of phyB (Fig. 1a) also plays a role in red light sensitivity via the modulation of thermal reversion *in vivo* using lines expressing multiple nonphosphorylatable (S to A) or phosphomimic (S to D) amino acid substitutions at S3 and S23-25 positions. The S3/23-25A and S3/23-25D quadruple mutations were combined with the S86A or S86D mutations to obtain phyB[S3/23-25/86A] and phyB[S3/23-25/86D] quintuple mutants to test whether balancing the phosphorylation status along the NTE is important for phyB activity. Although the phyB[S3/23-25A] mutant had a WT-like response in red light corresponding to a WT-like Pfr/Ptot value, the hypersensitive phyB[S86A] mutant phenotype was suppressed in the phyB[S3/23-25/86A] mutant that still had higher Pfr/Ptot compared with phyB (Fig. 6d,f). The phosphomimic phyB[S3/23-25D] mutant was hyposensitive in red light compared with WT phyB but had normal Pfr/Ptot. The phyB[S3/23-25/86D] mutant had reduced light responsiveness comparable to phyB[S86D], reflected by a strongly decreased Pfr/Ptot (Fig. 6d,f). Taken together, these data indicate that phosphorylation at S86 plays a dominant role in regulating phyB thermal reversion, but phosphorylation at S23-25 affects red light signaling, presumably by other pathways independent of thermal reversion.

The phosphorylation of Y104 was shown to affect light sensitivity dramatically (Nito *et al.*, 2013), but we wanted to know whether it affects the thermal reversion of phyB. We found that the phosphomimic phyB[Y104E] shows accelerated thermal reversion kinetics and reduced steady-state Pfr/Ptot, whereas nonphosphorylatable phyB[Y104F] had no effect on thermal reversion *in vivo* (Fig. S8).

The phyB D453R mutation enhances red light sensitivity through reduced thermal reversion

It has been shown that the kinase activity and the integrity of the ATP binding residue in the N-terminal photosensory domain of oat phyA are necessary for phyA function and the oat phyA [D422R] mutant exhibited strong defects in ATP binding and kinase activity (Shin *et al.*, 2016). Although the ATP-binding site and kinase activity of *Arabidopsis* phyB remain to be identified *in planta*, we tested whether the equivalent residue D453 at the N-terminal domain of phyB is important for phosphorylation and signaling. *Arabidopsis* seedlings expressing phyB[D453R] fused to YFP at physiological levels were hypersensitive in red light (Figs 7a, S7). Light sensitivity was even further enhanced compared with phyB[S86A], although expression levels were lower than in the control lines (Fig. 7a,b). Consistent with that, phyB [D453R] established higher Pfr/Ptot under nonsaturating red light irradiation (1 μmol m^{-2} s^{-1}), indicating a very slow thermal reversion (Fig. 7c). Our quantitative MS analyses demonstrate that the fragment containing residues S23, S24, S25, T27 was hyperphosphorylated in phyB[D453R] compared with phyB, whereas S86 phosphorylation remained unchanged (Fig. 7d). As the D453R mutation did not abolish phyB phosphorylation at the NTE, we concluded that D453 is not essential for the proposed autophosphorylation activity of phyB, but it seems to have a specific effect on S23–S25/T27 phosphorylation. Alternatively, D453R mutation could affect thermal reversion of phyB independently of NTE phosphorylation.

It is interesting that the phyB[G564E] mutant, having the mutation also in the PHY domain, has extremely slow thermal reversion (*phyB-401*) (Kretsch *et al.*, 2000; Ádám *et al.*, 2011). This phyB molecule did not exhibit hyperphosphorylation; instead its phosphorylation pattern at S86 and S23-25/T27 was no longer light-dependent (Fig. 7e). It is plausible that the mutant cannot distinguish between night and day as a result of highly stable Pfr form.

Discussion

PhyB is an excellent light quality and quantity sensor that can detect even subtle changes in light conditions. Thermal reversion is an intrinsic property of the phyB molecule that can be extensively modulated by intramolecular interactions and external factors (Viczián *et al.*, 2017). Hence, manipulating the thermal reversion rate represents an efficient mechanism to change red light sensitivity of the system. In this context, our results corroborate the findings of Medzihradszky *et al.* (2013) nicely and, in addition, demonstrate that the phosphomimic phyB[S86D] mutant alters phyB-mediated red light sensitivity by reducing physiologically active Pfr concentrations as a result of strongly accelerated thermal reversion of the Pfr–Pr heterodimer (k_{r1}). The fast reversion rate, k_{r1}, of the Pfr–Pr heterodimer is the most critical parameter for the light sensitivity of phyB-mediated

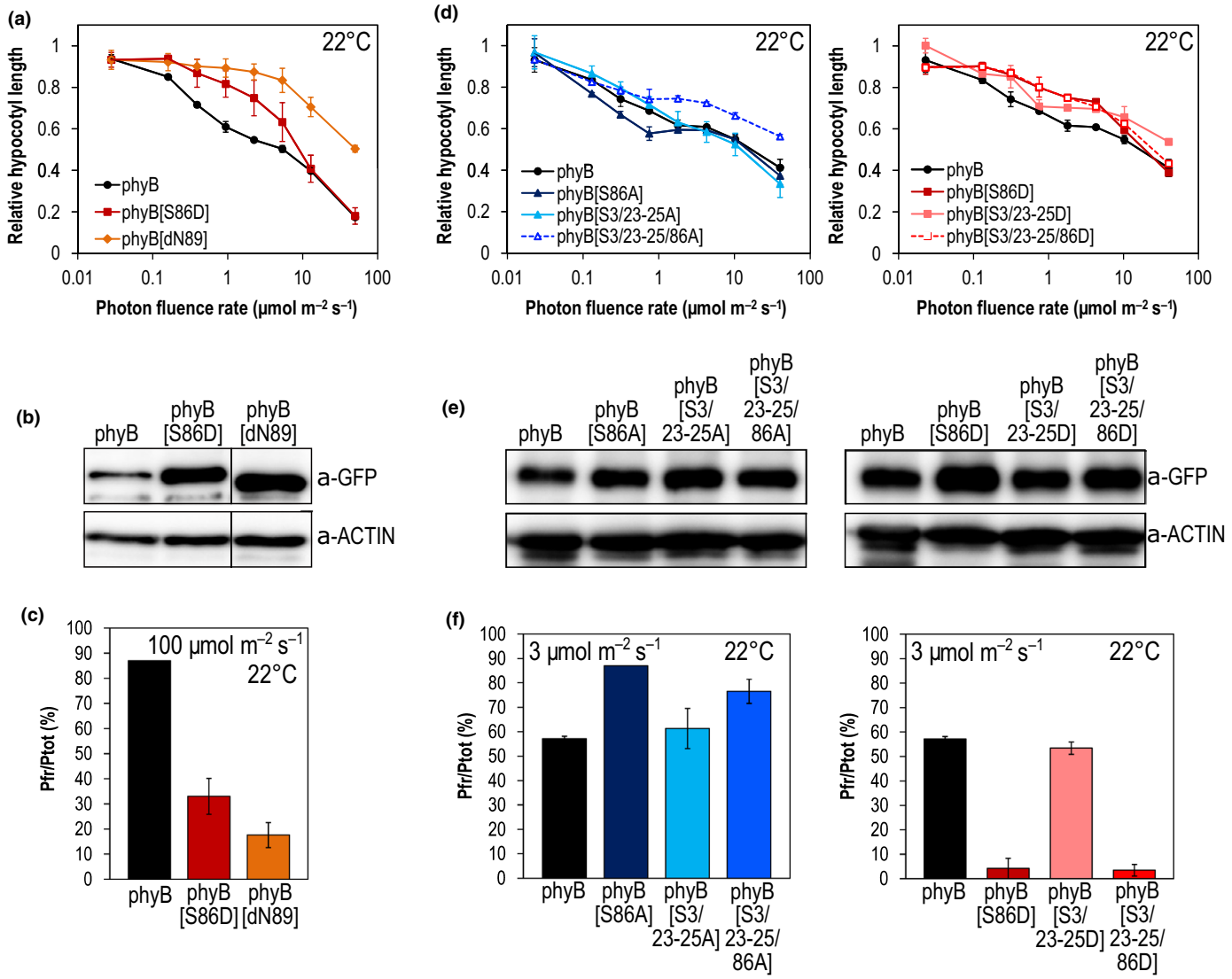

Fig. 6 N-terminal extension (NTE) deletion of phyB severely reduces concentrations of the far-red light-absorbing form (Pfr) of phyB, and additional phosphosites at the NTE influence red light sensitivity in *Arabidopsis thaliana*. (a, d) Fluence rate response curves for the inhibition of hypocotyl elongation in red light at 22°C. Seedlings expressing phyB-yellow fluorescent protein (phyB-YFP), phyB[S86D]-YFP or phyB[dN89]-YFP (a) and phyB[S86A]-YFP, phyB[S3/23-25A]-YFP or phyB[S3/23-25/86A]-YFP as well as phyB[S86D]-YFP, phyB[S3/23-25D]-YFP or phyB[S3/23-25/86D]-YFP (d) at physiological levels in the *phyB-9* mutant background were grown for 4 d in continuous red light. Relative hypocotyl lengths were calculated based on the length of the corresponding dark control. Data are means of two biological replicates with $n \leq 70$ seedlings. Error bars indicate SEM. (b, e) Immunoblot of total protein extracts from 4-d-old dark-grown seedlings of the transgenic lines used in (a, d). The phyB-YFP fusion proteins were detected using monoclonal anti-green fluorescent protein (anti-GFP) antibody. Actin was used as loading control. The composite image in (b) was assembled from the same membrane. (c, f) Pfr/Ptot ratios (Ptot, total amount of phytochrome) under steady-state conditions in red light at 22°C were measured by *in vivo* spectroscopy. Seedlings of transgenic lines with high expression of phyB[dN89]-YFP (c) and phyB[S3/23-25A]-YFP or phyB[S3/23-25/86A]-YFP and phyB[S3/23-25D]-YFP or phyB[S3/23-25/86D]-YFP (f) in the *phyB-9* mutant background were grown for 4 d in darkness and irradiated for 3 h with red light before measurement, to induce phyA degradation and establish the steady-state Pfr amounts. Seedlings overexpressing phyB-GFP, phyB[S86A]-YFP or phyB[S86D]-YFP were used as controls. Relative Pfr concentrations (%) are calculated based on the Ptot. Data are means of $n \geq 3$ independent measurements. Error bars indicate SEM.

responses (Klose *et al.*, 2015). Whereas k_{r2}, the thermal reversion rate of the Pfr–Pfr homodimers, is only increased two- to three-fold in the phyB[S86D] mutant, k_{r1} is increased about 50 times, causing strong reduction of the Pfr/Ptot ratios in light (Fig. 2e–i).

The S86 phosphorylation status changes dynamically *in vivo* in response to light and temperature, providing evidence for the capability of plants to modulate thermal reversion and consequently phyB activity via dynamic phosphorylation. High temperature and darkness, two conditions that reduce phyB activity, also enhanced S86 phosphorylation (Fig. 1c). However, this is not always reflected by the hypocotyl phenotypes: the difference in hypocotyl growth inhibition between WT phyB and phyB[S86A] was not increasing with temperature (Fig. 2a–c), although S86 phosphorylation was higher in WT phyB (Fig. 1c). This might be a result of the fact that only a small fraction of

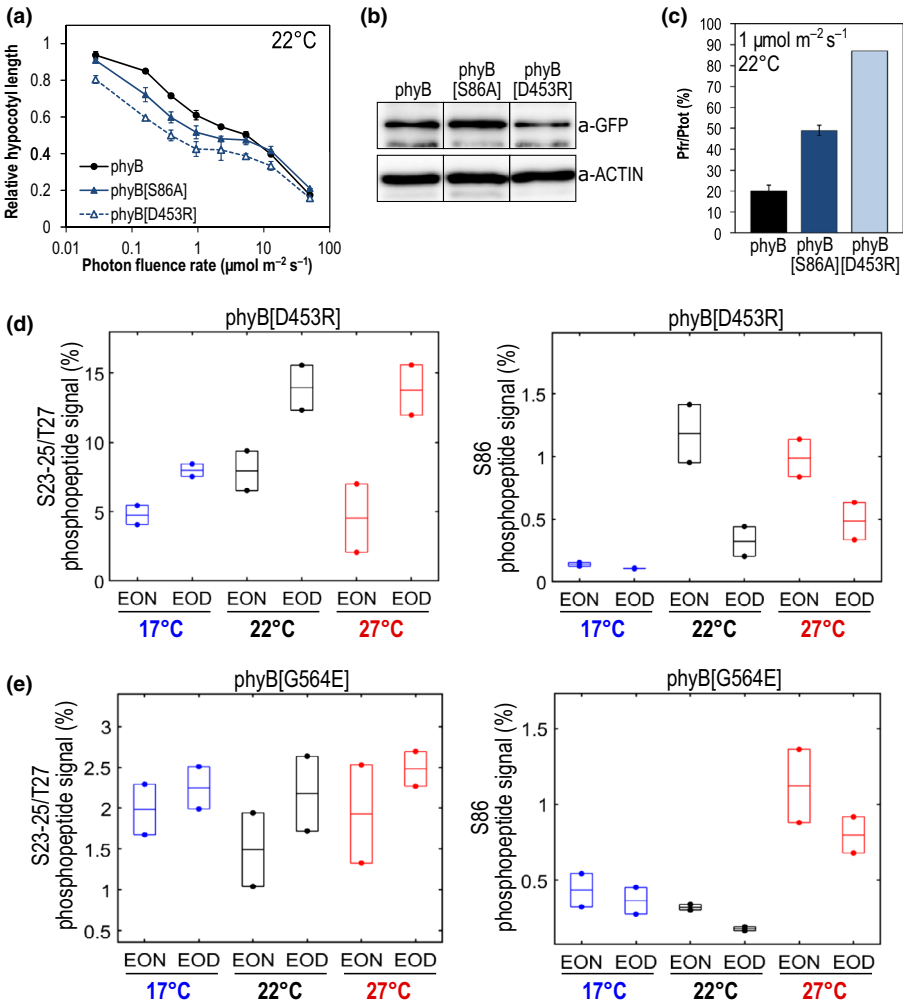

Fig. 7 The D453R mutation does not abolish phyB phosphorylation but enhances accumulation of the far-red light-absorbing form (Pfr) of phyB as well as red light sensitivity in *Arabidopsis thaliana*. (a) Fluence rate response curves for the inhibition of hypocotyl elongation in red light. Seedlings expressing phyB-yellow fluorescent protein (phyB-YFP), phyB[S86A]-YFP or phyB[D453R]-YFP at physiological levels in the *phyB-9* mutant background were grown for 4 d in continuous red light at 22°C. Relative hypocotyl lengths were calculated relative to the length of the dark control. Data are means of two biological replicates with $n \leq 70$ seedlings. Error bars indicate SEM. (b) Immunoblot of total protein extracts from 4-d-old dark-grown seedlings of the transgenic lines used in (a). The phyB-YFP fusion proteins were detected using monoclonal anti-green fluorescent protein (anti-GFP) antibody. Actin was used as loading control. The composite image was assembled from the same membrane. (c) Relative Pfr/Ptot ratios (Ptot, total amount of phytochrome) established under steady-state conditions in red light (1 µmol m^{-2} s^{-1}) at 22°C were measured by *in vivo* spectroscopy. Seedlings overexpressing phyB-GFP or phyB[S86A]-YFP and seedlings of a transgenic line with high phyB[D453R]-YFP expression in the *phyB-9* mutant were grown for 4 d in darkness and irradiated for 3 h with red light before measurement, to induce phyA degradation and establish the steady-state Pfr amounts. Relative Pfr concentrations (%) were calculated based on Ptot. Data are means of $n \geq 3$ independent measurements. Error bars indicate SEM. (d, e) Relative phosphopeptide signals corresponding to the fragments containing phosphorylated S23-25/T27 or phosphorylated S86 measured in phyB[D453R]-YFP- (d) or phyB[G564E]-YFP-expressing plants (e) grown in 12 h : 12 h light : dark cycles at the end of the dark cycle (EON) or at the end of the light cycle (EOD) under different temperatures (17, 22 and 27°C). Samples were analyzed as indicated in Fig. 1. Combined box- and scatterplots show the results of $n = 2$ biological replicates.

phyB is phosphorylated, which is not enough to cause a visible phenotype under the conditions used. Alternatively, S86 dephosphorylation in continuous light could compensate for the temperature-induced phosphorylation. In addition, the phosphorylation status of phyB could be balanced at multiple sites apart from S86 as shown for the S23-25/T27 fragment, which is phosphorylated in an opposite manner.

Whereas S86 is dephosphorylated in light, Pfr is progressively stabilized under continuous irradiation (Figs 1c, 3a-c). As there is no evidence that the photochemical reactions are affected by continuous irradiation, we conclude that Pfr stabilization in light is caused by a progressive reduction of the thermal reversion rate k_{r1}. Our data show that only a small percentage of the phyB pool is phosphorylated at a certain time point, and thus we believe that it is unlikely that S86 dephosphorylation is the only mechanism accounting for the observed Pfr stabilization. It was proposed that Pfr is stabilized through interaction with other proteins and is protected from thermal reversion within PBs (Sweere *et al.*, 2001; Rausenberger *et al.*, 2010; Klose *et al.*, 2015; Enderle *et al.*, 2017). Among these proteins, PHOTOPERIODIC CONTROL

OF HYPOCOTYL 1 (PCH1) and its homolog PCHL (PCH1-like), which accumulate in light and colocalize with phyB in PBs, were shown to inhibit phyB thermal reversion upon phyB binding (Huang *et al.*, 2016; Enderle *et al.*, 2017). Furthermore, a very recent study demonstrated that PCH1 stabilizes phyB Pfr *in vitro* and that PCH1 is an essential structural component of phyB PBs (Huang *et al.*, 2019). We found that the phyB molecules, mutated at phosphorylated residues and exhibiting thermal reversion phenotype, show no impaired binding to PCH1 and PCHL (Fig. S9). This result suggests that the role of PCH1 and PCHL in the regulation of phyB thermal reversion is not based on their binding ability to differently phosphorylated phyB molecules and both pathways act independently in the regulation of Pfr stability.

It remains to be determined how S86 phosphorylation enhances phyB thermal reversion mechanistically. In general, the NTE of phyB is assumed to be important for thermal stability of the Pfr form. Removal of the NTE from the phyB protein accelerated thermal reversion of phyB PSM fragments *in vitro* and abolished phyB localization to PBs in *Arabidopsis* (Chen *et al.*, 2005; Burgie *et al.*, 2014; Burgie *et al.*, 2017). Here, we provide photobiological and physiological evidence that NTE deletion severely enhances thermal reversion of phyB *in planta*, leading to very low Pfr concentrations even in high light, thus strongly reducing phyB activity (Fig. 6a–c). Until recently there was no structural information about phyB NTE available, as the published crystal structure of Arabidopsis phyB PSM lacks the NTE (Burgie *et al.*, 2014). Lately, a state-dependent interaction between the chromophore and the NTE in phyB was demonstrated by Raman spectroscopy (Velázquez Escobar *et al.*, 2017). Deletion of the NTE affected the chromophore and its surrounding hydrogen bonding network, particularly in the Pfr state, which could potentially affect the thermal reversion kinetics, and it was also revealed that the NTE undergoes light-dependent structural changes particularly in the S84–K88 region (Horsten *et al.*, 2016). Phosphorylation of residues in this region could lead to steric hindrance of the Pfr form, explaining the increased thermal reversion of the phosphomimic phyB[S86D] mutant of phyB. Although the effect of NTE deletion on thermal reversion of phyB is very pronounced, we cannot exclude the possibility that mutations in this region or NTE deletion might affect the photochemical properties of phyB and in that way contribute to the reduced red light sensitivity of the phyB[dN89] mutant.

As phosphorylation of PCSM residues was previously shown to regulate phyB signaling negatively (Nito *et al.*, 2013), it was proposed that phosphorylations at the PCSM motif promote rapid thermal reversion *in planta*, although direct experimental evidence was only available for S86 (Medzihradszky *et al.*, 2013). In contrast to the phosphomimic S86D mutant, which only partially impaired phyB signaling, a phosphomimic phyB[Y104E] was unable to complement the *phyB* mutant phenotype (Nito *et al.*, 2013). Here we demonstrate that phyB[Y104E] does indeed have strongly accelerated thermal reversion, but we observed that the nonphosphorylated phyB[Y104F] mutant exhibited a WT-like thermal reversion kinetics *in vivo* (Fig. S8). Interestingly it was found that a phyB[Y104A] mutant also has accelerated thermal reversion *in vitro* (Burgie *et al.*, 2014). Structural analyses revealed that an α-helix formed by residues Y104-R110 connects the NTE with the PAS domain and sterically shields the chromophore with Y104 directly adjoining the chromophore (Burgie *et al.*, 2014; Horsten *et al.*, 2016). Several studies demonstrate that glutamate is not always an effective mimetic for phosphotyrosine, as it has little chemical and structural similarity (Honda *et al.*, 2011; Chen & Cole, 2015); thus additional studies are needed to draw conclusions from tyrosine-phosphomimics.

The packing model between the NTE and the PSM predicts an intimate interaction between the PCSM and the light-sensing knot region which resembles the putative PIF binding site (Kikis *et al.*, 2009; Horsten *et al.*, 2016). Therefore, it is conceivable that the mechanism for inactivation of phyB signaling by phosphorylation involves blocking of the PIF binding capability of phyB. The Y104E mutation completely abolished Pfr-dependent PIF3 binding in an *in vitro* assay (Nito *et al.*, 2013) and the N-terminal fragment carrying S86D mutation only had a weakened interaction with PIF3 in yeast that could be compensated by using higher red light intensity (Medzihradszky *et al.*, 2013). As both phosphomimic mutants have failed to accumulate to high Pfr concentrations in light, it is also possible that the phosphorylation affects PIF3 binding indirectly via reducing the amount of phyB Pfr molecules available for binding.

The large NTE is unique to phyB and its paralog phyD. Whereas phosphorylation at the PCSM promotes rapid thermal reversion, dynamic phosphorylation at the more N-terminal residues S23-25/T27 did not affect thermal reversion of phyB *in vivo* but could modulate phyB activity by other, as yet unknown mechanisms (Fig. 6d–f). In line with this, sequential deletion of the N-terminal 50 amino acids of phyB, which are more or less absent in phyA, phyC and phyE, was shown to have little impact on thermal reversion *in vitro* (Burgie *et al.*, 2017). Taken together, our data show that phosphorylation also occurs in the PCSM of phyD and phyE *in vivo*, that it affects phyD- and phyE-mediated red light sensitivity and accelerates phyE thermal reversion (Fig. 5). This provides further evidence that the mechanism by which phosphorylation in the PCSM region inactivates red light signaling is common for all light-stable phytochromes.

We detected different phyB phosphorylation patterns in response to light and temperature, implying the activity of specific kinases and phosphatases. Several phosphatases were shown to interact with phytochromes (Kim *et al.*, 2002; Ryu *et al.*, 2005; Phee *et al.*, 2008) and furthermore phytochromes have been shown to act as autophosphorylating serine/threonine kinases. In oat phyA, autophosphorylation sites were identified residing in the NTE and a residue critical for ATP binding in the photosensory domain is necessary for kinase activity (Han *et al.*, 2010; Shin *et al.*, 2016). Our data show that these findings obtained for oat phyA are not directly conferrable to phyB. Mutating the corresponding residue in phyB, which is critical for ATP binding in phyA, did not abolish phosphorylation at the NTE but rather induced hyperphosphorylation at S23-25/T27. It suggests that this position is not essential for ATP binding,

autophosphorylation or to activate other kinases to phosphorylate phyB. Considering the different modes of action for phyA and phyB, it is not surprising that specific phosphorylation or dephosphorylation could be regulated differentially or could have different effects on phytochrome activity and signaling.

The control of phytochrome phosphorylation status represents a vital mechanism for fine-tuning the light responsiveness mediated by phytochromes. Whereas photochemical reactions are dominant under strong light, the thermal reversion rate k_{r1} becomes increasingly important for phyB Pfr steady-state concentrations as irradiance decreases, for example, under canopy shade, in cloudy days and/or at the extremes of the natural photoperiod (Klose *et al.*, 2015; Sellaro *et al.*, 2019). The impact of thermal reversion is also enhanced by high temperatures (Jung *et al.*, 2016; Legris *et al.*, 2016). Thus the phosphorylation status becomes physiologically most relevant in plants exposed to deep shade and high temperatures (Fig. 4). Therefore, the genetic modification of the S86 residue could offer a biotechnological target to adjust phyB sensitivity in a context of climate change without altering the ability of the photoreceptor to perceive the R : FR ratio.

Although the thermal reversion process has been known for decades, we are just starting to understand how it affects signaling and how it is modulated *in planta* to regulate plants' responsiveness to environmental stimuli. It is now understood that thermal reversion is regulated by a number of molecular mechanisms, including intra- as well as intermolecular interactions and post-translational modifications, but it is not clear how the different mechanisms are integrated. Further investigations are needed to reveal how these pathways are integrated in the regulation of Pfr thermal stability and red light sensitivity in Arabidopsis.

Acknowledgements

Work in Hungary was supported by the Hungarian Scientific Research Fund (OTKA, K-132633) and grants from the Economic Development and Innovation Operative Program (GINOP-2.3.2-15-2016-00001, GINOP-2.3.2-15-2016-00015 and GINOP-2.3.2-15-2016-00020). Work in Argentina was supported by the University of Buenos Aires (20020170100505BA) and ANPCYT (PICT-2016-1459). CK was supported by the Brigitte-Schlieben-Lange Fellowship of the Ministry of Science, Research and the Arts Baden-Wuerttemberg. Work in Germany was supported by the German Research Foundation (DFG) under Germany's Excellence Strategy (CIBSS – EXC-2189 – project ID 390939984 and BIOSS – EXC-294) and DGF grant HI-1369/7-1 to AH.

Author contributions

CK, AV, ES and FN planned and designed the research. AV, EA, AS, DL, EK, SRM and CK performed experiments and analyzed data. FN, AH, JC and CK supervised experimental work. JC analyzed data. CK and AV wrote the manuscript. CK, AV, FN, ES, JC and AH reviewed and edited the manuscript. FN, JC, CK and AH acquired funding. AV and ÉÁ contributed equally to this work.

ORCID

Jorge Casal https://orcid.org/0000-0001-6525-8414
Andreas Hiltbrunner https://orcid.org/0000-0003-0438-5297
Cornelia Klose https://orcid.org/0000-0003-0032-6556
Ferenc Nagy https://orcid.org/0000-0002-6157-9269
András Viczián https://orcid.org/0000-0003-2055-3430

References

Ádám É, Hussong A, Bindics J, Wüst F, Viczián A, Essing M, Medzihradszky M, Kircher S, Schäfer E, Nagy F. 2011. Altered dark- and photoconversion of phytochrome B mediate extreme light sensitivity and loss of photoreversibility of the phyB-401 mutant. *PLoS ONE* **6**: e27250.

Ádám É, Kircher S, Liu P, Mérai Z, González-Schain N, Hörner M, Viczián A, Monte E, Sharrock RA, Schäfer E *et al.* 2013. Comparative functional analysis of full-length and N-terminal fragments of phytochrome C, D and E in red light-induced signaling. *New Phytologist* **200**: 86–96.

Burgie ES, Bussell AN, Lye S-H, Wang T, Hu W, McLoughlin KE, Weber EL, Li H, Vierstra RD. 2017. Photosensing and thermosensing by phytochrome B require both proximal and distal allosteric features within the dimeric photoreceptor. *Scientific Reports* **7**: 13648.

Burgie ES, Bussell AN, Walker JM, Dubiel K, Vierstra RD. 2014. Crystal structure of the photosensing module from a red/far-red light-absorbing plant phytochrome. *Proceedings of the National Academy of Sciences, USA* **111**: 10179–10184.

Chen M, Tao Y, Lim J, Shaw A, Chory J. 2005. Regulation of phytochrome B nuclear localization through light-dependent unmasking of nuclear-localization signals. *Current Biology* **15**: 637–642.

Chen Z, Cole PA. 2015. Synthetic approaches to protein phosphorylation. *Current Opinion in Chemical Biology* **28**: 115–122.

Clough SJ, Bent AF. 1998. Floral dip: a simplified method for Agrobacterium-mediated transformation of *Arabidopsis thaliana*. *The Plant Journal* **16**: 735–743.

Enderle B, Sheerin DJ, Paik I, Kathare PK, Schwenk P, Klose C, Ulbrich MH, Huq E, Hiltbrunner A. 2017. PCH1 and PCHL promote photomorphogenesis in plants by controlling phytochrome B dark reversion. *Nature Communications* **8**: 2221.

Frosch S, Jabben M, Bergfeld R, Kleinig H, Mohr H. 1979. Inhibition of carotenoid biosynthesis by the herbicide SAN 9789 and its consequences for the action of phytochrome on plastogenesis. *Planta* **145**: 497–505.

Halliday KJ, Whitelam GC. 2003. Changes in photoperiod or temperature alter the functional relationships between phytochromes and reveal roles for phyD and phyE. *Plant Physiology* **131**: 1913–1920.

Han Y-J, Kim H-S, Kim Y-M, Shin A-Y, Lee S-S, Bhoo SH, Song P-S, Kim J-I. 2010. Functional characterization of phytochrome autophosphorylation in plant light signaling. *Plant & Cell Physiology* **51**: 596–609.

Honda M, Okuno Y, Yoo J, Ha T, Spies M. 2011. Tyrosine phosphorylation enhances RAD52-mediated annealing by modulating its DNA binding. *EMBO Journal* **30**: 3368–3382.

von Horsten S, Straß S, Hellwig N, Gruth V, Klasen R, Mielcarek A, Linne U, Morgner N, Essen L-O. 2016. Mapping light-driven conformational changes within the photosensory module of plant phytochrome B. *Scientific Reports* **6**: 34366.

Huang H, McLoughlin KE, Sorkin ML, Burgie ES, Bindbeutel RK, Vierstra RD, Nusinow DA. 2019. PCH1 regulates light, temperature, and circadian signaling as a structural component of phytochrome B-photobodies in Arabidopsis. *Proceedings of the National Academy of Sciences, USA* **116**: 8603–8608.

Huang H, Yoo CY, Bindbeutel R, Goldsworthy J, Tielking A, Alvarez S, Naldrett MJ, Evans BS, Chen M, Nusinow DA. 2016. PCH1 integrates circadian and light-signaling pathways to control photoperiod-responsive growth in Arabidopsis. *eLife* **5**: e13292.

Jabben M, Deitzer GF. 1978. A method for measuring phytochrome in plants grown in white light. *Photochemistry and Photobiology* **27**: 799–802.

Jabben M, Deitzer GF. 1979. Effects of the herbicide san 9789 on photomorphogenic responses. *Plant Physiology* **63**: 481–485.

Jung J-H, Domijan M, Klose C, Biswas S, Ezer D, Gao M, Khattak AK, Box MS, Charoensawan V, Cortijo S *et al.* 2016. Phytochromes function as thermosensors in Arabidopsis. *Science* **354**: 886–889.

Kikis EA, Oka Y, Hudson ME, Nagatani A, Quail PH. 2009. Residues clustered in the light-sensing knot of phytochrome B are necessary for conformer-specific binding to signaling partner PIF3. *PLOS Genetics* **5**: e1000352.

Kim D-H, Kang J-G, Yang S-S, Chung K-S, Song P-S, Park C-M. 2002. A phytochrome-associated protein phosphatase 2A modulates light signals in flowering time control in Arabidopsis. *Plant cell* **14**: 3043–3056.

Kircher S, Gil P, Kozma-Bognár L, Fejes E, Speth V, Husselstein-Muller T, Bauer D, Adám E, Schäfer E, Nagy F. 2002. Nucleocytoplasmic partitioning of the plant photoreceptors phytochrome A, B, C, D, and E is regulated differentially by light and exhibits a diurnal rhythm. *Plant Cell* **14**: 1541–1555.

Klement E, Gyula P, Viczián A. 2019. Detection of phytochrome phosphorylation in plants. *Methods in Molecular Biology* **2026**: 41–67.

Klose C. 2019. *In vivo* spectroscopy. *Methods in Molecular Biology* **2026**: 113–120.

Klose C, Venezia F, Hussong A, Kircher S, Schafer E, Fleck C. 2015. Systematic analysis of how phytochrome B dimerization determines its specificity. *Nature Plants* **1**: 15090.

Kretsch T, Poppe C, Schäfer E. 2000. A new type of mutation in the plant photoreceptor phytochrome B causes loss of photoreversibility and an extremely enhanced light sensitivity. *The Plant Journal* **22**: 177–186.

Lapko VN, Jiang XY, Smith DL, Song PS. 1997. Posttranslational modification of oat phytochrome A: phosphorylation of a specific serine in a multiple serine cluster. *Biochemistry* **36**: 10595–10599.

Lapko VN, Jiang XY, Smith DL, Song PS. 1999. Mass spectrometric characterization of oat phytochrome A: isoforms and posttranslational modifications. *Protein Science* **8**: 1032–1044.

Legris M, Klose C, Burgie ES, Rojas CCR, Neme M, Hiltbrunner A, Wigge PA, Schäfer E, Vierstra RD, Casal JJ. 2016. Phytochrome B integrates light and temperature signals in Arabidopsis. *Science* **354**: 897–900.

McMichael RW, Lagarias JC. 1990. Phosphopeptide mapping of Avena phytochrome phosphorylated by protein kinases *in vitro*. *Biochemistry* **29**: 3872–3878.

Medzihradszky M, Bindics J, Ádám É, Viczián A, Klement É, Lorrain S, Gyula P, Mérai Z, Fankhauser C, Medzihradszky KF *et al.* 2013. Phosphorylation of phytochrome B inhibits light-induced signaling via accelerated dark reversion in Arabidopsis. *Plant Cell* **25**: 535–544.

Nagatani A. 2010. Phytochrome: structural basis for its functions. *Current Opinion in Plant Biology* **13**: 565–570.

Nito K, Wong CC, Yates JR, Chory J. 2013. Tyrosine phosphorylation regulates the activity of phytochrome photoreceptors. *Cell Reports* **3**: 1970–1979.

Phee B-K, Kim J-I, Shin DH, Yoo J, Park K-J, Han Y-J, Kwon Y-K, Cho M-H, Jeon J-S, Bhoo SH *et al.* 2008. A novel protein phosphatase indirectly regulates phytochrome-interacting factor 3 via phytochrome. *The Biochemical journal* **415**: 247–255.

Qiu Y, Pasoreck EK, Reddy AK, Nagatani A, Ma W, Chory J, Chen M. 2017. Mechanism of early light signaling by the carboxy-terminal output module of Arabidopsis phytochrome B. *Nature Communications* **8**: 1905.

Quail PH. 2002. Phytochrome photosensory signalling networks. *Nature Reviews Molecular Cell Biology* **3**: 85–93.

Rausenberger J, Hussong A, Kircher S, Kirchenbauer D, Timmer J, Nagy F, Schäfer E, Fleck C. 2010. An integrative model for phytochrome B mediated photomorphogenesis: from protein dynamics to physiology. *PLoS ONE* **5**: e10721.

Reed JW, Nagatani A, Elich TD, Fagan M, Chory J. 1994. Phytochrome A and phytochrome B have overlapping but distinct functions in Arabidopsis development. *Plant Physiology* **104**: 1139–1149.

Reed JW, Nagpal P, Poole DS, Furuya M, Chory J. 1993. Mutations in the gene for the red/far-red light receptor phytochrome B alter cell elongation and physiological responses throughout Arabidopsis development. *Plant Cell* **5**: 147–157.

Rockwell NC, Su Y-S, Lagarias JC. 2006. Phytochrome structure and signaling mechanisms. *Annual Review of Plant Biology* **57**: 837–858.

Ryu JS, Kim J-I, Kunkel T, Kim BC, Cho DS, Hong SH, Kim S-H, Fernández AP, Kim Y, Alonso JM *et al.* 2005. Phytochrome-specific type 5 phosphatase controls light signal flux by enhancing phytochrome stability and affinity for a signal transducer. *Cell* **120**: 395–406.

Sánchez-Lamas M, Lorenzo CD, Cerdán PD. 2016. Bottom-up assembly of the phytochrome network. *PLOS Genetics* **12**: e1006413.

Sellaro R, Smith RW, Legris M, Fleck C, Casal JJ. 2019. Phytochrome B dynamics departs from photoequilibrium in the field. *Plant, Cell & Environment* **42**: 606–617.

Shin A-Y, Han Y-J, Baek A, Ahn T, Kim SY, Nguyen TS, Son M, Lee KW, Shen Y, Song P-S *et al.* 2016. Evidence that phytochrome functions as a protein kinase in plant light signalling. *Nature Communications* **7**: 11545.

Smith H. 2000. Phytochromes and light signal perception by plants–an emerging synthesis. *Nature* **407**: 585–591.

Sweere U, Eichenberg K, Lohrmann J, Mira-Rodado V, Bäurle I, Kudla J, Nagy F, Schafer E, Harter K. 2001. Interaction of the response regulator ARR4 with phytochrome B in modulating red light signaling. *Science* **294**: 1108–1111.

Velázquez Escobar F, Buhrke D, Fernandez Lopez M, Shenkutie SM, von Horsten S, Essen L-O, Hughes J, Hildebrandt P. 2017. Structural communication between the chromophore-binding pocket and the N-terminal extension in plant phytochrome phyB. *FEBS letters* **591**: 1258–1265.

Viczián A, Klose C, Ádám É, Nagy F. 2017. New insights of red light-induced development. *Plant, Cell & Environment* **40**: 2457–2468.

Wagner D, Tepperman JM, Quail PH. 1991. Overexpression of phytochrome B induces a short hypocotyl phenotype in transgenic Arabidopsis. *Plant Cell* **3**: 1275–1288.

Yamaguchi R, Nakamura M, Mochizuki N, Kay SA, Nagatani A. 1999. Light-dependent translocation of a phytochrome B-GFP fusion protein to the nucleus in transgenic Arabidopsis. *Journal of Cell Biology* **145**: 437–445.

Yeh KC, Lagarias JC. 1998. Eukaryotic phytochromes: light-regulated serine/threonine protein kinases with histidine kinase ancestry. *Proceedings of the National Academy of Sciences, USA* **95**: 13976–13981.

Zhang S, Li C, Zhou Y, Wang X, Li H, Feng Z, Chen H, Qin G, Jin D, Terzaghi W *et al.* 2018. TANDEM ZINC-FINGER/PLUS3 is a key component of phytochrome A signaling. *Plant Cell* **30**: 835–852.

Zhou Y, Yang L, Duan J, Cheng J, Shen Y, Wang X, Han R, Li H, Li Z, Wang L *et al.* 2018. Hinge region of Arabidopsis phyA plays an important role in regulating phyA function. *Proceedings of the National Academy of Sciences, USA* **115**: E11864–E11873.

Supporting Information

Additional Supporting Information may be found online in the Supporting Information section at the end of the article.

Fig. S1 Additional data from independent transgenic phyB mutant lines (corresponding to Fig. 2).

Fig. S2 Temperature-dependent thermal reversion kinetics.

Fig. S3 phyB photobody formation is enhanced in prolonged continuous red light irradiation.

Fig. S4 Additional data from independent transgenic phyD and phyE mutant lines (corresponding to Fig. 5).

Fig. S5 Expression and subcellular localization of phyD-YFP and its mutant versions in transgenic *Arabidopsis* seedlings.

Fig. S6 Expression and subcellular localization localization of phyE-YFP and its mutant versions in transgenic *Arabidopsis* seedlings.

Fig. S7 Additional data from independent transgenic phyB mutant lines (corresponding to Figs 6, 7).

Fig. S8 Thermal reversion kinetics of the phyB Y104 mutants.

Fig. S9 The phyB mutant versions are not impaired in binding PCH1 or PCHL in a yeast two-hybrid growth assay.

Methods S1 Detailed description of the experimental procedures used in this study.

Notes S1 MS/MS protein spectra of phosphorylated phyB peptides.

Notes S2 MS/MS protein spectra of phosphorylated phyD and phyE peptides.

Table S1 Transgenic *Arabidopsis* lines used in this study.

Table S2 List of oligonucleotides used for cloning.